

N O T I C E

THIS DOCUMENT HAS BEEN REPRODUCED FROM
MICROFICHE. ALTHOUGH IT IS RECOGNIZED THAT
CERTAIN PORTIONS ARE ILLEGIBLE, IT IS BEING RELEASED
IN THE INTEREST OF MAKING AVAILABLE AS MUCH
INFORMATION AS POSSIBLE

NASA Technical Memorandum 81703

(NASA-TM-81703) PERFORMANCE OF A MAGNETIC
MULTIPOLE LINE-CUSP ARGON ION THRUSTER
(NASA) 12 F HC A02/MF A01 CSCL 21C

N81-19219

Unclass

G3/20 41630

Performance of a Magnetic Multipole Line-Cusp Argon Ion Thruster

James S. Sovey
Lewis Research Center
Cleveland, Ohio



Prepared for the
Fifteenth International Electric Propulsion Conference
cosponsored by the American Institute of Aeronautics and Astronautics,
the Japan Society for Aeronautical and Space Sciences,
and Deutsche Gesellschaft für Luft- und Raumfahrt
Las Vegas, Nevada, April 21-23, 1981

NASA

PERFORMANCE OF A MAGNETIC MULTIPOLE LINE-CUSP ARGON ION THRUSTER

James S. Sovey
National Aeronautics and Space Administration
Lewis Research Center
Cleveland, Ohio 44135

Abstract

A 17-cm diameter line-cusp ion thruster was evaluated with inert gases which are candidate propellants for on-orbit and orbit transfer propulsion functions for Large Space Systems. A semi-empirical relationship was generated to predict thruster beam current in terms of plasma parameters which would allow initial thruster optimization without ion extraction and the associated large vacuum facilities. The sensitivity of performance to changes in discharge electrode configurations and magnetic circuit was evaluated and is presented. After final optimization a propellant utilization efficiency of 0.9 at a discharge chamber power expenditure of about 260 W per beam ampere was obtained. These performance parameters are the highest yet achieved with argon propellant.

Introduction

Inert gas ion thrusters are being considered for orbit transfer and on-orbit propulsion functions for Large Space Systems. Inert gases are attractive propellants because they are plentiful and should minimize the ecological impact of the propulsion systems. The inert gas systems should also allow for easy integration with the Space Transportation System and spacecraft.

System analyses have been performed for inert gas systems and have shown that thruster performance strongly impacts such key mission parameters as trip time and power requirements.⁽¹⁾ A number of performance-related investigations have dealt with component and discharge optimization of thrusters employing divergent⁽²⁾ and multipole^(3,4,5,6) magnetic field discharge chambers. The multipole magnetic confinement schemes generally tend to improve primary electron confinement, increase plasma density and uniformity, and increase inert gas propellant utilization efficiency when compared with divergent field thrusters. Discharge losses, with argon propellant, of about 300 W per beam ampere (W/A)⁽⁴⁾ and 400 W/A⁽⁵⁾ at a propellant utilization efficiency of 0.75 have been reported for such multipole discharge chambers.

This paper describes the characteristics of a magnetic multipole line-cusp discharge chamber. The line-cusp differs from other magnetic circuits in the arrangement of the magnets which provide the electron confinement. The line-cusp magnetic circuit has been previously employed in nonthruster applications.⁽⁷⁾ These ion sources have produced uniform argon, hydrogen, and deuterium plasmas at relatively high plasma densities.^(8,9)

Basic optimization of the thruster discharge chamber was performed without ion extraction by the use of plasma probes to measure ion density. This procedure permitted the use of smaller vacuum facilities and power supplies. Optimization procedures included variation of the line-cusp magnetic circuit, anode position, and cathode position to yield the highest ion density. Finally, the thruster per-

formance was further documented with ion extraction using a high-performance, dished ion optics assembly.

Apparatus and Procedure

A section view of the reference thruster, which resulted from optimization without ion extraction, is shown in Fig. 1. The chamber inside diameter, determined by the magnets, was 20 cm. The magnetic circuit was composed of 20 magnet rows which alternated in polarity and produced 20 line-cusps spaced about 3.2 cm apart. Samarium-cobalt magnets whose dimensions were 2.5x2.5 by 1.1 cm long were used. When placed in the magnetic circuit, the magnet field strength at the surface was 0.3 T. The mild steel shell was water cooled to maintain the magnet temperature less than 200° C. The samarium-cobalt magnets showed irreversible field strength losses of a few percent at 220° C and had up to 50 percent losses at 320° C.

The reference thruster cathode was placed about 23 cm from the downstream end of the shell. As shown in Fig. 1 there were no pole pieces in the cathode region in order to reduce potential ion loss areas. The optimum axial magnetic field strength at the cathode was found to be about 18 mT (Fig. 2(a)). In order to produce an 18-mT field at the cathode as well as low axial field at the ion optics, the magnets were specially arranged in the cone. For example, a "North" magnet row had three magnets extended into the cone while a "South" magnet row had only one magnet extended into the cone (Fig. 1). The magnetic field had rather steep spatial gradients such that the volume within about 8 cm of the ion optics had radial and axial field strengths of less than 2 mT except near the boundary anodes (Fig. 2).

The cathode primary electrons travel through the weakly diverging field region into a relatively field free volume where strong fields exist only at the boundary anodes. The reference thruster had 10 tubular anodes 1.2 cm diameter by 20 cm long which were placed between alternating rows of magnets. Figure 3 shows the end view of the line-cusp thruster without a screen grid mask. Most of the optical excitation was contained within a 14-cm diameter which was the distance between opposite anodes (Fig. 1). After a series of optimization procedures, the anodes were positioned radially such that the azimuthal magnetic field at the anode internal extremity (14 cm diam) would be 14.5 and 12.5 mT, respectively, at locations 19 and 3.5 cm from the downstream end of the shell.

Argon flow was admitted through a 6.4-mm diameter hollow cathode⁽²⁾ and through a perforated tube located at the upstream end of the discharge chamber. The hollow cathode orifice (0.76 mm diameter) was chamfered and had a 0.5-mm long throat. The downstream end of the cathode was fitted with a 17-mm diameter by 0.8-mm thick tantalum radiation fin. Other parts of the assembly are a barium impregnated porous tungsten cathode insert and a swaged tantalum heater. Discharge ignition was ac-

complished by applying a 3-kV, 3 μ sec pulse between a wire electrode and the cathode. After the gas breakdown the discharge coupled between the cathode and tubular anodes.

When ions were extracted, a dished ion optical system with screen and accelerator grid open area fractions of 0.75 and 0.27, respectively, was used.⁽¹⁰⁾ The grid-to-grid spacing was set to about 0.7 mm. The 30-cm diameter ion optics were mounted to a 31-cm diameter stainless-steel shell. The screen grid was masked using tantalum foil to diameters ranging from 14 to 17 cm diameter. For all tests the grids were operated at +1000 and -500 V.

A 6.4-mm diameter hollow cathode neutralizer was used along with an enclosed keeper electrode spaced 1.2 cm from the cathode.⁽²⁾ The neutralizer tip was located 10 cm axially and 17 cm radially from the last row of accelerator grid holes. The neutralizer flow rate was about 0.4 equivalent amperes of argon. Because the neutralizer did not perform efficiently at beam currents exceeding 1 A, neutralization was by both the active hollow cathode and secondary electrons emitted from vacuum facility surfaces which were impinged upon by ions.

Initial discharge chamber optimization and ion density measurements were performed without ion extraction. This procedure was employed because a vacuum facility with modest pumping capability could be used; only two thruster power supplies were required, and test turn-around time was rapid. During this activity effects of anode radial position and cathode position were examined and the magnetic circuit in the truncated cone region was defined. Held fixed were the number of rows of magnets (20) and the number of anodes (10). The thruster configuration resulting from these optimization procedures was referred to as the reference thruster. During the initial optimization without ion extraction, plasma parameters were measured with a Langmuir probe which consisted of a 0.5-mm diameter tungsten wire with a 5.1-mm length exposed to the plasma. The wire was supported by two concentric alumina tubes. The probe was located on the thruster centerline about 1 centimeter from a perforated plate which was used to simulate the ion optics' gas impedance.

Next, the thruster was operated in a 4.6-m diameter by 19.2-m long vacuum facility with ion extraction. These tests were undertaken to determine the performance sensitivity of parameters which included screen mask diameter, anode radial position, number of anodes, number of magnet rows, anode length, and thruster length. The vacuum facility was capable of operating at 7×10^{-6} torr while handling 3 A of argon flow. Gas flow rates were measured with mass flow rate transducers which were calibrated using volume displacement methods. The cathode flow rate, usually about 0.55 A, was selected to yield a discharge voltage of 45 to 50 V at a discharge current of 22 A.

Results and Discussion

The results of procedures and tests to improve the ionization and gas efficiency of an inert gas thruster are presented herein. A thruster length-to-diameter ratio in excess of one was chosen in order to increase the propellant utilization efficiency which was generally limited to less than 0.80 in previous efforts.^(2,4,5) The line-cusp magne-

tic circuit with multiple anodes was selected with the intention of improving primary electron confinement, plasma density, and beam uniformity.^(7,8,9) The effects of varying magnetic circuit and chamber geometry was documented with ion extraction after first-order optimization efforts were made using plasma probe diagnostics without ion extraction.

Discharge Chamber Performance without Ion Extraction

In order to obtain the largest beam diameter with a 22.5-cm diameter iron shell, 20 rows of magnets with 3.2 cm cusp spacings were selected for the initial experiment. The 20 magnet row configuration reduced field penetration into the center of the chamber (Fig. 2(b)). Given a 22.5-cm diameter shell and a magnet width of 2.5 cm the maximum number of magnet rows, allowing some space for anode mounts, was 20. Ten rather than 20 anodes were used due to space limitations for the anode mounting insulators. Initial tests dealt with the variation of the anode radial position to establish discharge impedance and ion current density sensitivities. It was found that when the magnetic field at the anode internal extremity was increased, both the discharge impedance and the probe ion current increased if the flow rates and discharge power were held constant.

When the magnetic field over the anodes was increased to 15 mT the discharge was difficult to start and undesirably high impedance modes were encountered for most combinations of cathode and main discharge argon flow rates. When the magnetic field over the anode internal extremity was reduced to 12.6 mT, there was no difficulty starting the discharge, the discharge impedance was lower, and the plasma probe ion current increased slightly at a given discharge power. However, voltage excursions in the V-I characteristic still existed (Fig. 4(a)).

Discharge chambers without magnets in the cone region exhibited undesirable peaks in the discharge V-I characteristic that were sometimes in excess of 80 V and could limit the discharge current depending upon the power supply voltage capability. The data in Fig. 4 show the effect of extending magnets into the truncated cone region of the thruster and alternating the number of magnets per row. This change produced a monotonically increasing V-I discharge characteristic. Furthermore, by placing magnets in the cone the probe ion current increased by 20 to 80 percent depending upon the value of discharge power selected for comparison purposes. There was a slight increase in the azimuthal magnetic field over the anodes at the upstream end of the shell. More importantly, the axial magnetic field strength at the cathode tip changed from about 0.2 to 18 mT. The effect of axial magnetic field strength in the region of the cathode was examined more carefully during tests with ion extraction.

The effect of varying cathode position on the discharge chamber ion density was also investigated. The cathode was placed at five different positions which were 20 to 27 cm from the downstream end of the shell (Fig. 1). The discharge voltage was between 46 and 49 V, at a 20-A cathode discharge current, for all cathode positions except the 20-cm position where the discharge voltage was about 42 V. The highest probe ion current was obtained at a cathode position between 22 and 23 cm upstream of the end of the shell. Retracting the cathode from the 20- to the 23-cm position resulted in about a

20-percent increase in probe ion current. As seen from Fig. 2(a), the 23-cm position was slightly upstream of the maximum axial magnetic field strength. This type of position was found to be preferred in the optimization of a cesium thruster.⁽³⁾ The cathode was finally positioned 23 cm upstream of the end of the shell prior to final documentation with a Langmuir probe.

Measurements from a negatively biased cylindrical probe provided guidance in the optimization procedures concerning magnetic circuit, anode position, and cathode position. Prior to performing tests with ion extraction, measurements of electron temperature, plasma potential, and plasma density were made using the reference thruster whose prominent characteristics are shown in table I. Based on previous results,⁽⁴⁾ it was felt that the thrusters yielding ion densities in excess of $2 \times 10^{11} \text{ cm}^{-3}$ would also provide high performance with ion extraction. The data of Fig. 5 indicate that the ion densities range from $2 \times 10^{11} \text{ cm}^{-3}$ to about $5 \times 10^{11} \text{ cm}^{-3}$ as the discharge power varied from 200 to 900 W. In this case the total and cathode argon neutral flow rates were about 2 and 0.5 A, respectively. The Langmuir probe characteristics were linear on the usual semi-logarithmic plot indicating a Maxwellian distribution of electrons in the vicinity of the screen grid. Electron temperatures were in the range 6 to 8 eV. In all cases plasma potential was 1 to 3 V positive with respect to anode potential. The thruster configuration resulting from this series of tests is documented in table I.

Performance with Ion Extraction

Tests with ion extraction were carried out in the 4.6-m diameter vacuum facility. Gas flow corrections for facility gas ingestion into the thruster were less than 1 percent for argon flow rates used. Argon flow rates were generally less than 3 A. No attempt was made to correct the discharge propellant utilization efficiency or discharge chamber losses for multiple ionized species. The degree of multiple ionization was limited by adjusting the cathode to main discharge argon flow rate ratio such that the discharge voltage for the data reported herein was generally less than 50 V.

The performance of the reference thruster was evaluated with an ion optical system having screen and accelerator grid open area fractions of 0.75 and 0.24, respectively. The data of Fig. 5(b) indicate that the ion density obtained without extraction and the ion beam current have nearly identical shape functions when plotted against discharge power. In both cases the downstream grid open area was about 60 cm^2 . At 670 W discharge power, the ion number density obtained without ion extraction was about $4.3 \times 10^{11} \text{ cm}^{-3}$. When the thruster was operated with ion extraction, at slightly higher flow rates, the resulting beam current was 2.15 A or an average beam current density of 9.5 mA/cm^2 . Typical performance parameters for argon using the reference thruster were 275 W of discharge power per beam ampere at a propellant utilization efficiency of 0.9 and a discharge voltage of about 40 V. Beam currents of 2.9 A and average ion current densities of 13 mA/cm^2 have been obtained with the 17-cm diameter thruster. The data also indicate that relatively high-performance line-cusp thrusters may be obtained by optimization procedures without ion extraction, using plasma probes.

From Fig. 5(b) a semi-empirical relationship can be generated to predict the maximum beam current of magnetic multipole thrusters using ion density and electron temperature values measured without ion extraction. The plasma parameters were measured on the thruster centerline about 1 cm from the screen grid. Using the usual ion flux parameters, the Bohm ion velocity,⁽⁶⁾ and the experimentally determined factor of 0.46, the maximum beam current becomes:

$$J_B = \alpha A_s n_i e \left(\frac{kT_e}{m_i} \right)^{1/2} \quad (1)$$

where

J_B	ion beam current, A
α	0.46, proportionality constant
A_s	Screen grid open area, m^2
n_i	ion density, m^{-3}
e	electronic charge, $1.6 \times 10^{-19} \text{ C}$
k	$1.38 \times 10^{-23} \text{ J/K}$
T_e	electron temperature, K
m_i	ion mass, kg

Ion beam currents have previously been estimated by using 1.0 for α .⁽⁶⁾ Other authors have used $0.5 < \alpha < 0.6$ for analogous equations dealing with plasma probe ion collection.⁽¹¹⁾ Equation (1), with $\alpha = 0.46$, matches the experimental data of Fig. 5(b) to within ± 7 percent (Fig. 6). Because the ion density and electron temperatures were measured on the thruster centerline near the screen grid, the α value accounts for variations in the radial ion density. In the reference thruster, for example, the probe ion currents were 94 percent and about 66 percent of the centerline value at one-half and full ion extraction radius, respectively. The discharge V-I characteristics of Fig. 5(a), with and without ion extraction, are not identical and the plasma properties probably differ to some extent so it is not clear at the time how accurately Eq. (1) could be extended to other magnetic multipole ion sources.

Figure 7 shows the discharge chamber performance of the reference thruster with both argon and xenon. The minimum energy expenditure for both gases was about 200 W/A. The effective discharge chamber length-to-diameter ratio was greater than 1.3. This parameter was tailored to increase argon performance. Thus the reported xenon discharge chamber losses are higher than would exist for a chamber specifically designed for xenon.

The maximum argon propellant utilization efficiency, uncorrected for multiply-charged ions, shown in Fig. 7 was about 0.98 at 340 W/A and a discharge voltage of 46.3 V. The maximum apparent propellant utilization efficiency for xenon was greater than one. If it is assumed that Xe^+ and Xe^{++} are the only ions that comprise the beam current, then at least 23 percent of the total beam current was Xe^{++} at a discharge voltage of 38.5 V and an average ion beam current density of 11 mA/cm^2 .

In order to limit multiply-charged ion production, discharge voltages for argon and xenon were kept below 50 and 40 V, respectively. With this guideline in mind, the hollow cathode flow rates required to produce the lowest discharge chamber losses were about 0.65 and 0.13 A for argon and xenon, respectively.

In an attempt to lower the discharge chamber power losses, the cylindrical chamber length was reduced by approximately 7.5 cm. The short thruster configuration had three less magnets per row than the reference thruster (table I). Curve 1 of Fig. 8(a) shows the resulting axial magnetic field strength. The discharge chamber performance was rather poor and resulted in a high discharge voltage, low ion production situation (Fig. 8(c)). Thus, decreasing the length of the line-cusp thruster required reconfiguration of the axial magnetic field gradient. These data, as well as the data taken without ion extraction, indicate that the axial magnetic field and field gradient in the region of the hollow cathode play an important role in the ion production rate.

The magnets in the cone region of the thruster were reconfigured to produce a total of six different axial magnetic field profiles which are shown in Figs. 8(a) and (b). Figures 8(a) and (c) show that if the magnetic field strength in the region of the cathode was less than 4 mT or if the magnetic field axial gradient was not proper, a high discharge voltage mode results or was accompanied by poor performance. The best performance was obtained (Figs. 8(b) and (c)) when the field strength at the cathode tip was between 17 and 37 mT and a rather steep field gradient existed near the cathode.

The discharge losses of the chamber shortened by 7.5 cm with a length-to-diameter ratio of 0.9, were 380 W/A at a propellant utilization efficiency of 0.9. These losses were about 100 W/A higher than obtained with the longer reference thruster whose effective length-to-diameter ratio was about 1.3. Performance comparison of the thruster lengths may have been compromised since the magnetic field at the extremity of the anodes was about 10 mT in the case of the short thruster versus 12.5 mT for the reference thruster. The data of Fig. 8 do, however, display the importance of selecting the appropriate magnetic field and field gradient in the region of the cathode.

A series of tests were undertaken to lower discharge losses and determine the sensitivity of performance to changes in discharge chamber parameters (table II). For ease of presentation all performance comparisons were made at a propellant utilization efficiency of 0.9. By increasing the screen grid mask diameter from about the internal anode extremity (15 cm diam) to 17 cm diameter, the discharge losses were decreased by about 60 W/A. Figure 3 shows significant optical excitation between anodes and thus it might be expected that this region would also have relatively high ion production as well.

The anode placement in the magnetic field was also varied in three different situations. The magnetic field at the anode internal extremity, at locations 19 and 3.5 cm from the downstream end of the iron shell, were set to 10/10, 14.5/12.5, and 20/12.5 mT. The reference thruster, which had the intermediate magnetic field values, exhibited dis-

charge losses that were 9 and 27 percent lower than the respective thruster configurations with the high and low magnetic fields. The magnetic field over the anodes of the reference thruster produced a primary electron diffusion parameter, $(6) \int B dx$, of about 100×10^{-6} T-m which is the flux integral over the anode toward the thruster axis. The diffusion parameter is related to the electron current permitted to diffuse to anodes without the anodes becoming more positive than the plasma.

The flux integral of 100×10^{-6} T-m was also close to a semi-empirical guideline where $\int B dx$ in tesla meters should be approximately equal to 13.5×10^{-6} multiplied by the square root of the average primary electron energy in electron volts.⁽¹²⁾ This relationship was arrived at by simply considering primary electron deflection in a uniform strength magnetic field.

Attempts to reduce the number of anodes in the reference thruster from 10 to 6 or to decrease the length of the anode tubes by 38 percent resulted in increases in discharge losses of about 80 and 20 percent, respectively (table II). Discharge losses were reduced by 5 percent when $0.6 \times 0.6 \times 20$ cm iron strips were placed in the center of each row of magnets. The strips provided a more uniform magnetic field⁽⁷⁾ in the cusp region at the expense of an 8-percent lower magnetic field strength.

The sensitivity of discharge chamber performance to variation in the number of rows of magnets was examined using a fixed shell diameter of 22 cm (table II). The configurations investigated had 20, 16, and 12 rows of magnets with 10, 16, and 12 anodes, respectively. Relative cusp spacings for the three configurations were 3.2, 3.9, and 5.3 cm. Setting the magnetic field over the anodes at about 12.5 mT resulted in spacings between opposite anodes of 14, 12.7, and 11.8 cm for the chambers with 20, 16, and 12 rows of magnets, respectively. The 12-row magnetic configuration had a 15-cm diameter screen grid mask while the others had a 27-cm diameter mask. Results indicated that the reference thruster exhibited discharge losses at least 20 percent lower than the thrusters with 12 and 16 rows of magnets. Thus, the lowest discharge losses were obtained with the lowest cusp spacing, about 3 cm. The screen mask diameter for the 16-row magnetic configuration should probably have been reduced for a more accurate comparison, however.

Most line-cusp ion sources used by other investigators^(7,8,9) operate the shell as well as the magnets at anode potential. The discharge chamber performance of the reference thruster, modified to perform with 16 rows of magnets and 16 anodes, was compared to a chamber whose only difference was the elimination of the tube anodes and subsequent operation of the shell at anode potential. The discharge chamber losses of the thruster with the shell anode, 300 W/A at a propellant utilization efficiency (η_{pd}) of 0.9, were 26 percent lower than the configuration with 16 anode tubes, but 9 percent higher than the reference thruster (table II). However, the reference thruster configured to operate with a shell anode had discharge chamber losses 16 percent higher than the basic reference thruster at $\eta_{pd} = 0.9$. Further efforts to reduce discharge chamber losses should include multiple anode configurations as well as the simple geometry of the shell anode thruster.

Some of the argon thruster configurations were constructed such that the screen grid and iron shell

assembly could be electrically isolated and negatively biased to measure ion currents. The screen grid ion current was about 18 percent of the total ion flux at the grid plane. Thus the effective screen grid transparency was a minimum of 82 percent versus a geometrical transparency of 75 percent. For the reference thruster the shell ion currents were 0.8 and 1.7 A at beam currents of 1.4 and 2.7 A, respectively. The fact that shell ion currents of about 60 percent of the beam current exist in the reference thruster implies the base-level discharge losses could be reduced to below 160 W/A by devising efficient ion confinement schemes that would reduce ion wall losses by 50 percent.

Conclusions

The performance of a 17-cm diameter line-cusp ion thruster was evaluated using argon and xenon propellants. Basic optimization of the thruster was accomplished without ion extraction so that performance tests could be conducted with smaller vacuum facilities and power supplies. Based on these tests, a semi-empirical relationship was generated to predict thruster beam current in terms of discharge plasma parameters.

The sensitivity of performance to changes in discharge electrode configurations and magnetic circuit was evaluated. It was found that both an axial magnetic field strength of about 18 mT at the cathode tip and a rather steep axial field gradient were required to assure a monotonically increasing V-I discharge characteristic and high ion density. For best results the cathode was positioned near the maximum of the axial magnetic field. It was also determined that better argon thruster performance was obtained for an effective discharge chamber length to diameter ratio of 1.3 versus one with a ratio of 0.9. Lowest discharge chamber losses were obtained when the magnetic field strength tangent to the tube anode at the internal extremity was about 12 mT. After final optimization an argon propellant utilization efficiency of 0.9, at 260 W of discharge power per beam ampere, was obtained with a thruster with 20 rows of magnets and 10 tubular anodes. These performance parameters are the highest yet achieved with argon propellant. The average ion beam current densities were as high as 13 mA/cm².

Argon line-cusp thrusters with either tube anodes or a shell anode yielded discharge losses between 260 and 320 W/A at 0.9 propellant utilization efficiency. Both anode configurations should be considered in future thruster optimization effort. Considerable improvement in thruster efficiency may be possible because the ion side wall losses were as much as 60 percent of the beam current.

References

1. Byers, D. C., "Characteristics of Primary Electric Propulsion Systems," AIAA Paper 79-2041, Oct. 1979.
2. Sovey, J. S., "Characteristics of a 30-Cm Diameter Argon Ion Source," AIAA Paper 76-1017, Nov. 1976.
3. Moore, R. D., "Magneto-Electrostatically Contained Plasma Ion Thruster," AIAA Paper 69-260, Mar. 1969.
4. Ramsey, W. D., "12-Cm Argon/Xenon Ion Source," *Journal of Spacecraft and Rockets*, Vol. 16, No. 4, July-Aug. 1979, pp. 252-257.
5. Kaufman, H. R., "Inert Gas Thrusters," Colorado State Univ., Fort Collins, CO, Nov. 1978. (NASA CR-159527.)
6. Kaufman, H. R. and Robinson, R. S., "Plasma Processes in Inert Gas Thrusters," AIAA Paper 79-2055, Oct. 1979.
7. Forrester, A. T., Goebel, D. M., and Crow, J. T., IBIS - "A Hollow-Cathode Multipole Boundary Ion Source," *Applied Physics Letters*, Vol. 33, No. 1, July 1978, pp. 11-13.
8. Stirling, W. L., Ryan, P. M., Tsai, C. C., and Leung, K. N., "Magnetic Multipole Line-Cusp Plasma Generator for Neutral Beam Injectors," *Review of Scientific Instruments*, Vol. 50, No. 1, Jan. 1979, pp. 102-108.
9. Ehlers, K. W. and Leung, K. N., "Characteristics of the Berkeley Multicusp Ion Source," *Review of Scientific Instruments*, Vol. 50, No. 11, Nov. 1979, pp. 1353-1361.
10. Rawlin, V. K., "Sensitivity of 30-Cm Mercury Bombardment Ion Thruster Characteristics to Accelerator Grid Design," AIAA Paper 78-668, Apr. 1978.
11. de Leeuw, J. H., "Electrostatic Plasma Probes," *Physico-Chemical Diagnostics in Plasmas, Proceedings Fifth Biennial Gas Dynamics Symposium*, T. P. Anderson, R. W. Springer, and R. C. Warder, Jr., eds., Northwestern University Press, Evanston, IL, 1963, pp. 65-95.

TABLE I. - REFERENCE THRUSTER CONFIGURATION

C, Length of cylindrical shell	23 cm
G, Screen grid diameter.	17 cm
D, Distance between opposite anodes.	14 cm
A, Number of anode tubes	10
L, Anode length.	20.3 cm
R, Rows of magnets	20
N, North magnets per row	11
S, South magnets per row	9
M, Magnetic field over anodes (upstream/downstream).	14.5 mT/12.5 mT
B _z , Axial magnetic field at cathode.	19 mT

TABLE II. - SENSITIVITY OF PERFORMANCE TO CHANGES IN DISCHARGE CHAMBER GEOMETRY

Type of change	Parameters dissimilar from those of the reference thruster	Performance		
		Discharge voltage, V	ϵ at $\eta_{UD} = 0.9$ W/A	$\Delta\epsilon/\epsilon_{ref}, \eta_{UD} = 0.9$
No change	Reference thruster	40	275	0
Screen grid diameter	G = 15 cm	40.6	340	+0.24
Magnetic field at anode	M = 10/10 mT	43	350	+0.27
Magnetic field at anode	M = 20/12.5 mT	40	300	+0.09
Number of anodes	A = 6, m = 10/10 mT	>50	>500	>+0.82
Anode length	L = 12.5 cm, M = 13.5/12.5 mT	47	330	+0.20
Magnetic circuit	0.6x0.6x20 cm Iron strips placed on top of magnets in the cylinder	38.6	260	-0.05
Rows of magnets	R = 12, A = 12, D = 11.8 cm, B _z = 11 mT	42.5	370	+0.35
Rows of magnets	R = 16, A = 16, D = 12.7 cm, B _z = 21 mT	42	330	+0.20
Length of thruster	C = 15 cm, N = 7, S = 6, B _z = 17 mT, M = 9/9.5 mT	42	380	+0.38
Shell anode	A = 0, R = 16, B _z = 17 mT	42	300	+0.09
Shell anode	A = 0, B _z = 14 mT	42	320	+0.16
* η_{UD} : Discharge propellant utilization efficiency uncorrected for multiply-charged ions * ϵ : Discharge power per beam ampere, W/A * $\Delta\epsilon = \epsilon - \epsilon_{ref}$				

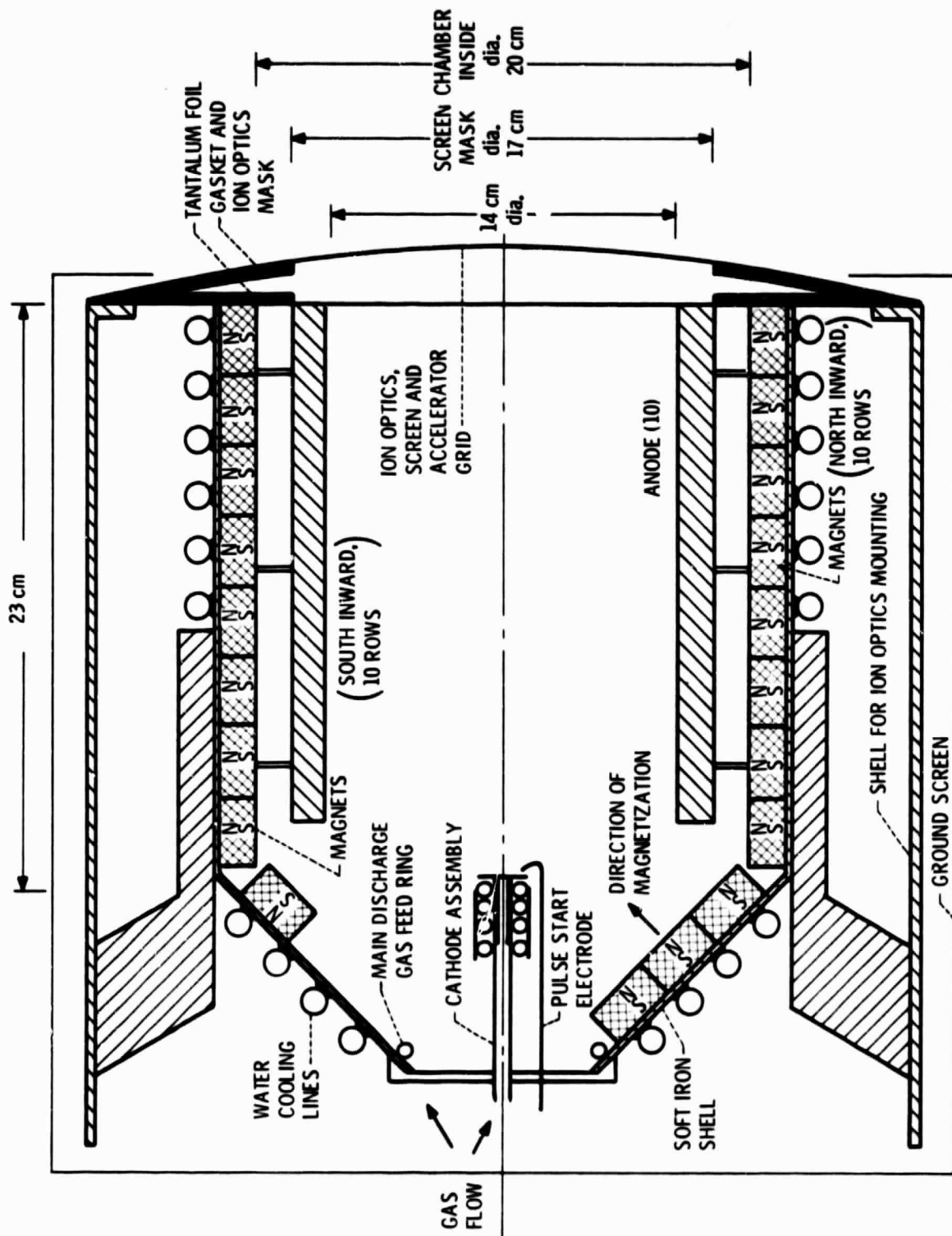


Figure 1. - Cross-section of reference thruster. Rows of magnets alternate polarity.

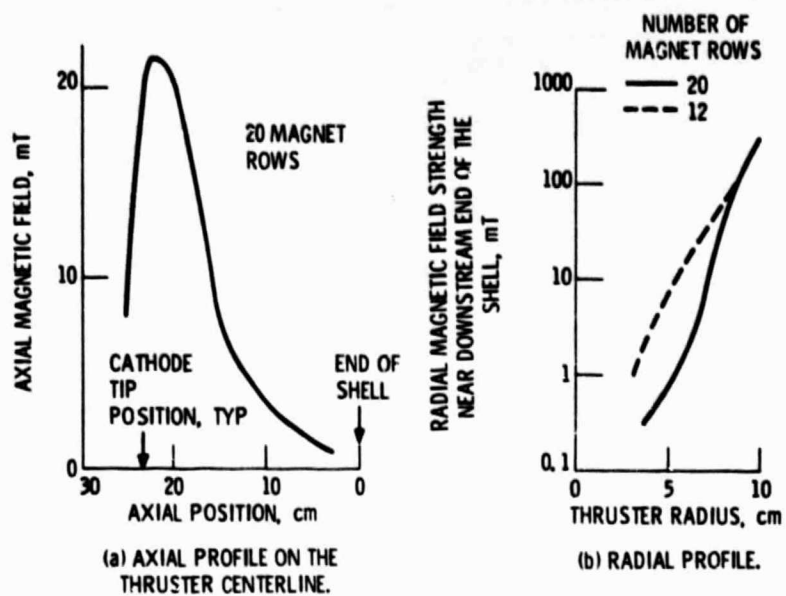


Figure 2 - Typical discharge chamber magnetic field profiles.

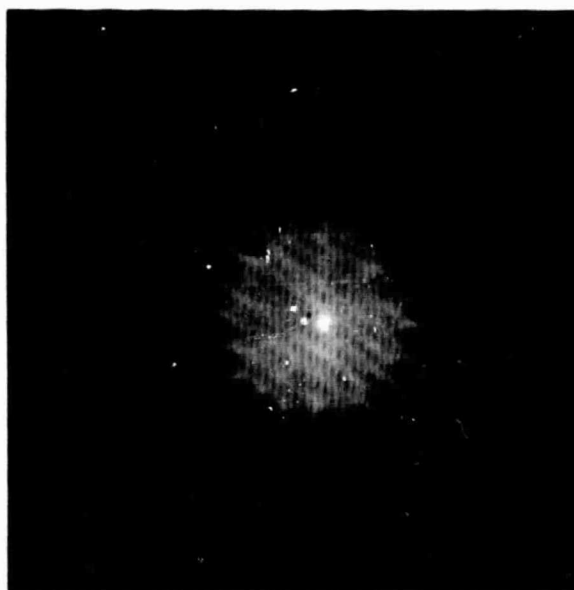


Figure 3 - Photograph of thruster operating without screen grid mask.

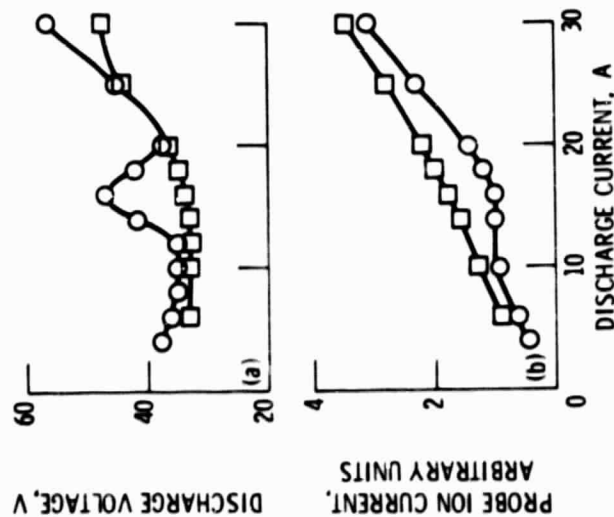
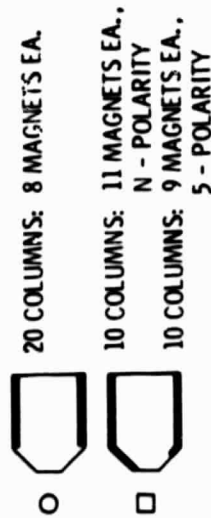


Figure 4. - Variation of probe ion current and discharge voltage with discharge current for cone chambers with and without magnets in the cone region. (No ion extraction: 10 anode tubes; magnetic field over anodes 14.5-12.5 mT)

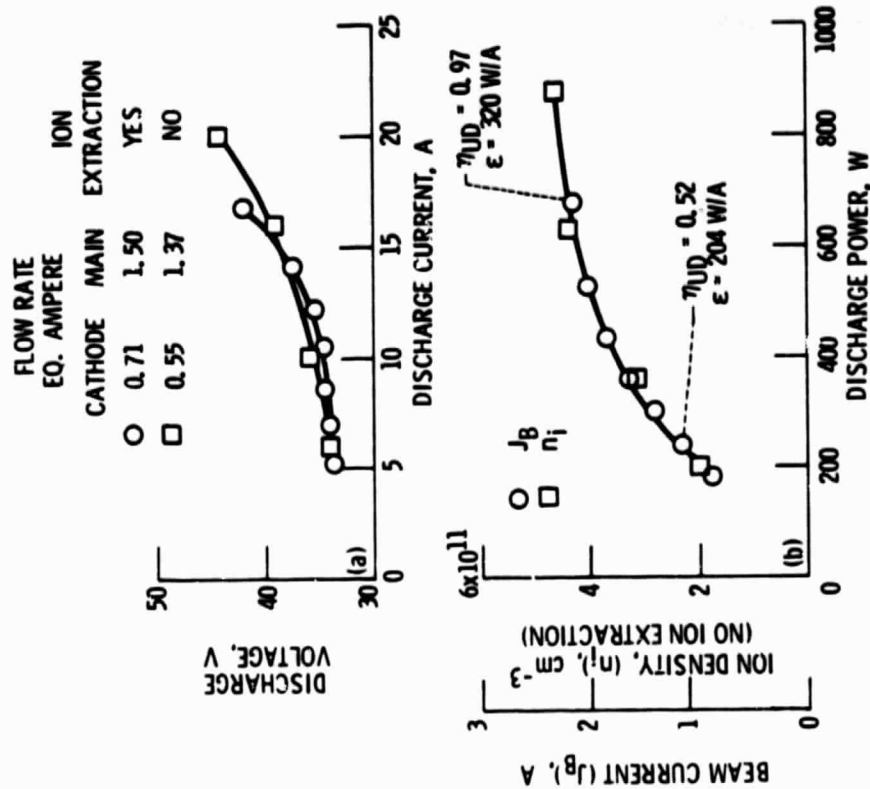


Figure 5. - Comparison of discharge, beam and plasma parameters with and without ion extraction. (η_{UD} : Discharge propellant utilization efficiency; ϵ : Discharge power per beam ampere, W/A)

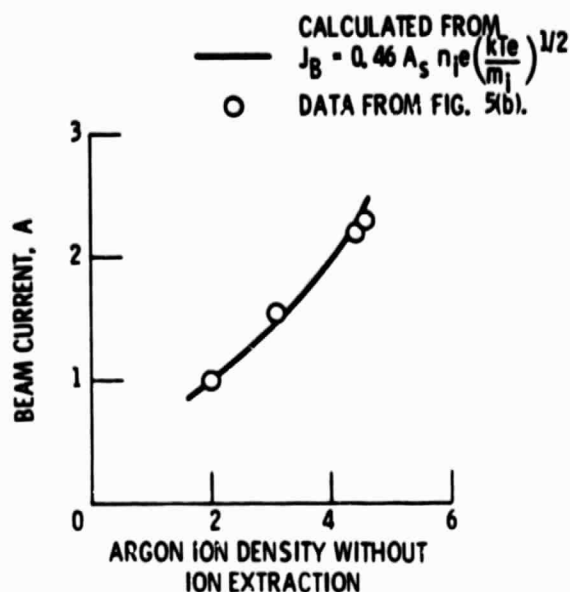


Figure 6. - Comparison of measured beam current versus the beam current calculated from plasma parameters without ion extraction. Screen grid open area = 170 cm^2 . $6 < \frac{kT}{e} < 8 \text{ eV}$ for the data of figure 5(b).

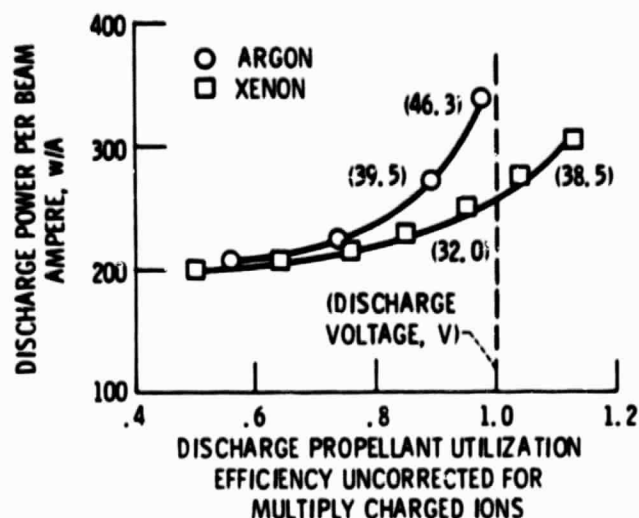


Figure 7. - Discharge chamber performance of the reference thruster. Cathode and total flowrates for argon and xenon were 0.65 A, 2.55 A and 0.13 A, 2.17 A respectively.

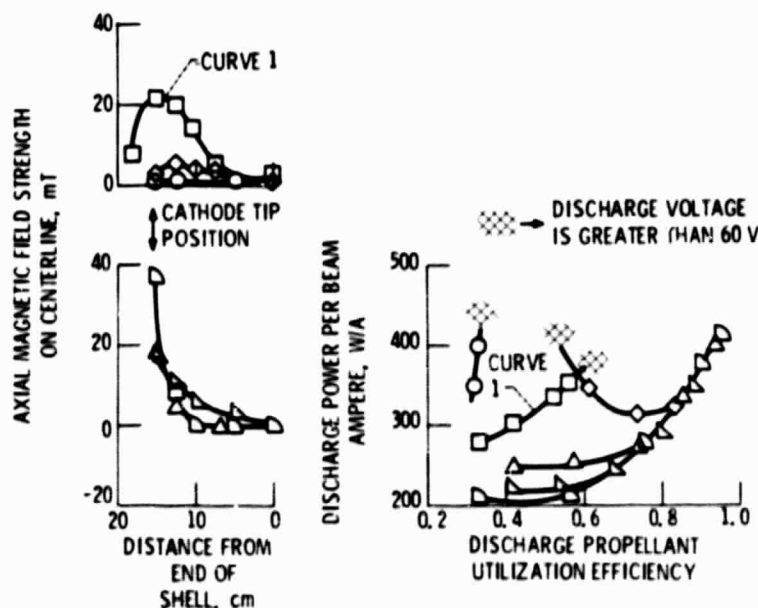


Figure 8. - Effect of axial magnetic field strength on discharge chamber performance. Argon flow rate 2.0 to 2.7 A. Shell cylinder length, 15 cm. Magnetic field over anodes, $\approx 10 \text{ mT}$.